

# Removal of Small-Molecular-Weight Organic Matter by Coagulation, Adsorption, and Oxidation: Molecular Transformation and Disinfection Byproduct Formation Potential

Mengjie Liu, Muhammad Saboor Siddique, Nigel J. D. Graham, and Wenzheng Yu\*



Cite This: <https://doi.org/10.1021/acsestengg.1c00409>



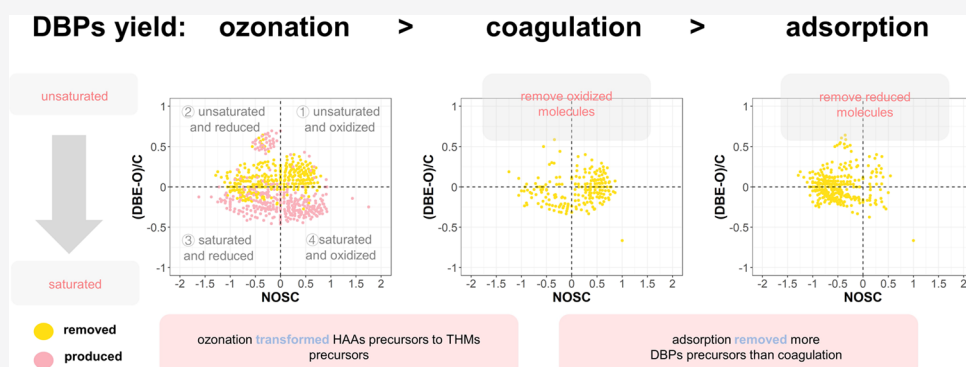
Read Online

ACCESS |

Metrics & More

Article Recommendations

Supporting Information



**ABSTRACT:** The removal of small-molecular-weight organic matter (SMW-OM) is important for enhancing final water quality and increasing the performance of unit processes. However, the fate of SMW-OM during drinking water treatments has received a few concerns. In this study, the performances of three common processes (coagulation, adsorption, and ozonation) on treating SMW-OM were comprehensively studied at a molecular scale. For molecules only containing C, H, and O elements, coagulation favored the removal of unsaturated structures (low H/C) with oxygen-containing groups (high O/C). While for N-containing molecules, those with higher H/C were better removed. Adsorption preferentially removed reduced molecules (low O/C) and can remove molecules with a very low mass (20% removal rate for molecules with a mass of 300–350 Da). Therefore, it showed the best performance on decreasing the disinfection byproduct formation potential (DBPFP). Ozonation had a limited mineralization effect on organic contents. In addition, it transformed haloacetic acid (HAA) precursors to trihalomethane (THM) precursors by degrading aromatic structures to aliphatic compounds (e.g., aldehydes and ketones), and thus resulted in an increase in the THM formation potential. This study focused on the fate of SMW-OM in drinking water treatment and their DBPFP, illustrated its transformation process, and can provide guidance for enhanced drinking water treatment in practical applications.

**KEYWORDS:** coagulation, adsorption, ozonation, small-molecular-weight organic matter, disinfection byproducts

## 1. INTRODUCTION

In the context of global shortages in water resources<sup>1,2</sup> and environmental pollution,<sup>3,4</sup> the demand for clean and healthy drinking water is of increasing importance. In conventional drinking water treatment, raw water goes through a series of unit processes in order to remove a range of contaminants, including natural organic matter (NOM). NOM with a large molecular weight (MW) mostly consists of biopolymers, which are easy to be removed from water by coagulation or ultrafiltration.<sup>5</sup> The residual NOM with a small MW, termed as SMW-OM in this study, represents a significant proportion of the organic content of the surface waters (~95%), and is the target contaminant in enhanced drinking water treatment. For instance, SMW-OM has been reported to cause rapid nanofiltration (NF) membrane fouling. In addition, the increasing concern of disinfection byproducts (DBPs) in

drinking water highlights the requirements to remove as much as DBP precursors (residual NOM) before chlorination. Therefore, maximizing the removal of SMW-OM is an important objective in enhanced drinking water treatment. However, the treatment of SMW-OM has received a few concerns, and there is no study evaluating the performance of different treatments on the removal of SMW-OM. In view of

Received: November 4, 2021

Revised: January 27, 2022

Accepted: January 28, 2022

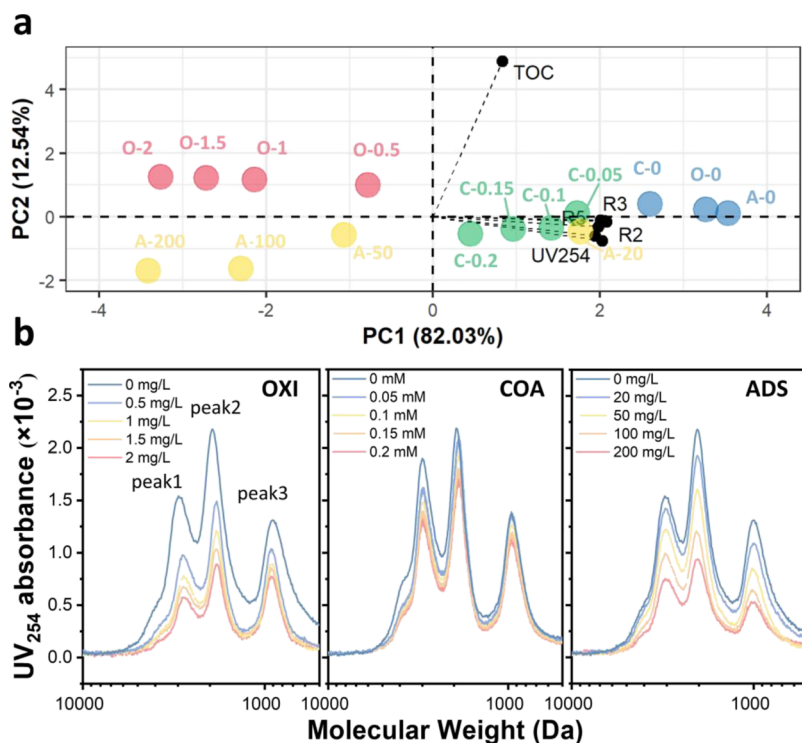


**Figure 1.** Water quality indexes of water samples before and after treatments. (a) PCA results of water samples, red, green, yellow, and blue represent oxidation (O), coagulation (C), adsorption (A), and JM samples, and the number represents the dosage of ozone,  $\text{Al}^{3+}$ , and PAC. Black points were water indexes: TOC, UV254, and five EEM regional integrated fluorescence intensity. R1: tyrosine-like aromatic protein; R2: tryptophan-like aromatic protein; R3: fulvic acid-like matter; R4: soluble microbial byproduct-like matter; and R5: humic acid-like matter; (b) MW distribution by SEC of oxidation (OXI), coagulation (COA), and adsorption (ADS).

the foregoing, it is necessary, and timely, to investigate the fate of SMW-OM during common water treatment processes.

The methods used to quantify and characterize NOM include total organic carbon (TOC) analysis, UV-visible spectroscopy (UV), three-dimensional (3D) excitation-emission matrix spectrofluorometry (EEM), size exclusion chromatography (SEC), and so forth, which indicate the mass concentration (as C), the chromophoric properties, the fluorescence properties, and the MW distribution of NOM components, respectively. Using these methods, previous studies have drawn some important conclusions concerning the variation of NOM composition during different water treatment processes.<sup>6–8</sup> However, these studies consider the nature organic matter (DOM) as a whole, and the treatment of SMW-OM after the removal of large-MW fractions has not been investigated. In addition, these manuscripts only study one process, and the performances, especially for DBP formation, were difficult to compare because they used different water sources with a distinct DOM composition.

The aim of this study is to systematically compare the performance of different treatments on the removal of SMW-OM and the reduction of DBP formation potential. Coagulation, adsorption, and ozonation were chosen because of their prevalence in water treatment. First, bulk characterizations (TOC, UV, EEM, and SEC) were used to show the performance and to determine the optimal doses of three treatments based on the consideration of both the effect and cost. Second, the effects of three treatments on reducing DBP precursors were evaluated. After that, high-resolution mass spectrometry was used to give a molecular insight into the transformations of SMW-OM during three treatments.<sup>9–11</sup>

The removed and produced molecules were identified and characterized to explain the variation of DBPFP. This study, focusing on the fate of SMW-OM in drinking water treatment and their DBPFP, illustrated its transformation process and can provide guidance for enhanced drinking water treatment in practical applications.

## 2. MATERIALS AND METHODS

**2.1. Raw Water and Treatments.** Samples of raw water were obtained from the JingMi (JM) river, Beijing, China, which is the channel providing water for industrial production, farmland irrigation, and domestic use.<sup>5</sup> The physical and chemical properties of JM river are shown in Table S3. The raw water was filtered successively through  $0.45\ \mu\text{m}$  and PES 20 kDa membranes to remove particulate substances and large-MW substances, respectively. The filtrate was referred to as JM water.

Aluminum sulfate ( $\text{Al}_2(\text{SO}_4)_3 \cdot 12\text{H}_2\text{O}$ ), obtained from Sinopharm Chemical Reagent Co. Ltd., and powdered activated carbon (PAC, 400 mesh) from Macklin, China, were used as the coagulant and adsorbent in the experiments. Ozone was generated from oxygen using an ozone generator (KRC Marine LTD, UK) and applied in the tests as the method of oxidation. All tests were conducted at room temperature ( $25 \pm 1^\circ\text{C}$ ), and the pH of JM water was  $7.75 \pm 0.03$ . The water samples after coagulation, adsorption, and oxidation were referred to as COA, ADS, and OXI, respectively. Water samples were stored at  $4^\circ\text{C}$  and restored to room temperature before use or measurement. More detailed information concerning the experimental procedures

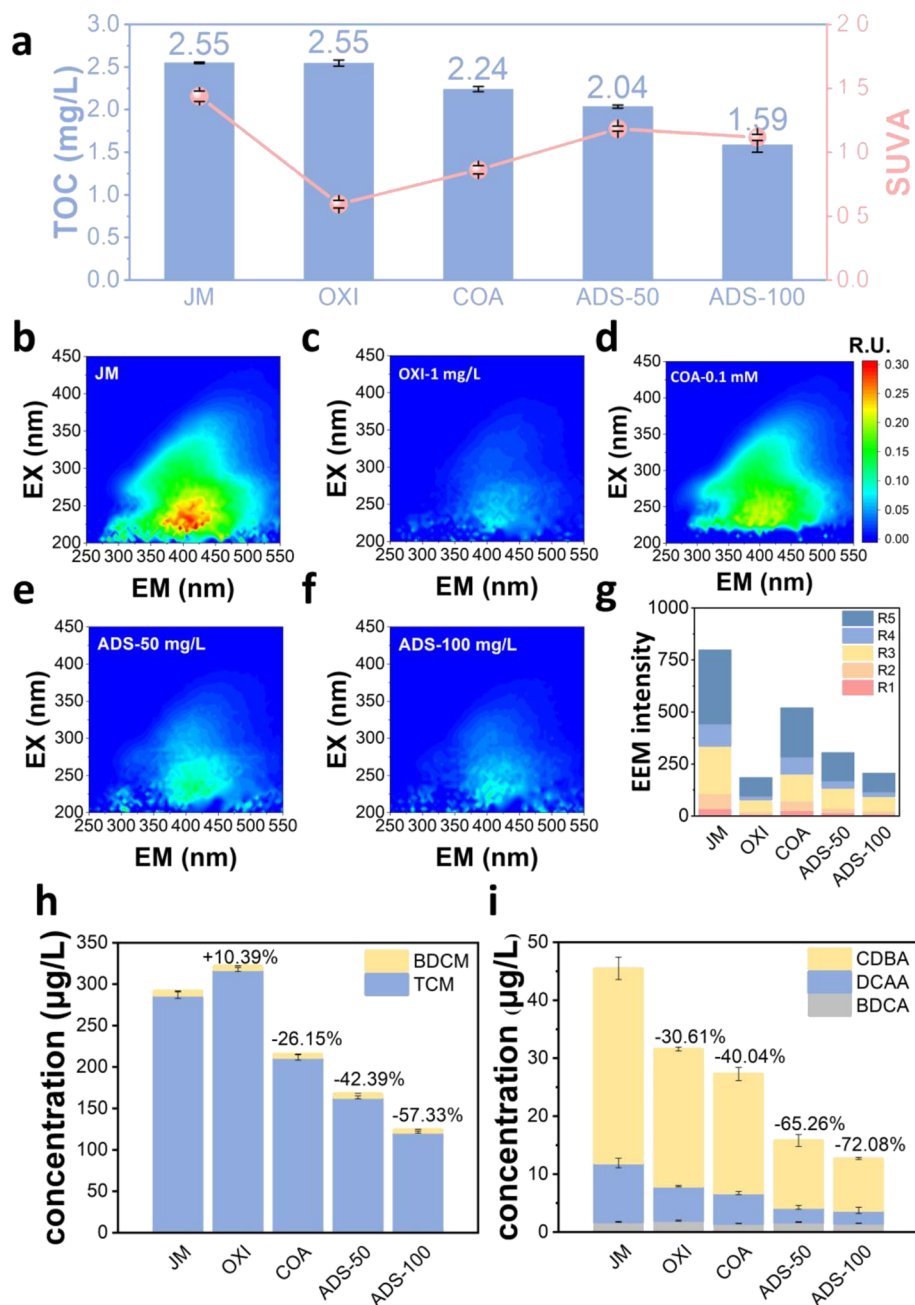


**Figure 2.** (a) TOC and SUVA; (b–f) EEM spectra; (g) EEM regional integrated fluorescence intensity. R1: tyrosine-like aromatic protein; R2: tryptophan-like aromatic protein; R3: fulvic acid-like matter; R4: soluble microbial byproduct-like matter; and R5: humic acid-like matter; (h, i) trihalomethanes (THMs); (h) haloacetic acids (HAAs) and (i) formation potentials. The number indicates the variation percentage of different treatments compared to JM. The abbreviations were bromodichloromethane (BDCM); trichloromethane (TCM); chlorodibromoacetic acid (CDBA); dichloroacetic acid (DCAA); and bromodichloroacetic acid (BDCA).

for ozonation, coagulation, adsorption (Text S1–3) is provided in the Supporting Information (SI).

**2.2. Analytical Methods.** A UV-visible spectrophotometer (UV-2600, Shimadzu, Japan) and 3D excitation-emission matrix (EEM) spectrofluorometer (F-4600FL, Hitachi, Japan) were used to characterize the chromophore and fluorescent organic substances in water samples, respectively. TOC was measured using a TOC analyzer (TOC-Vwp, Shimadzu, Japan), and the MW distribution was determined by SEC equipped with an optical detector (Waters, USA).

DBPFP was measured using a gas chromatograph (Clarus 590, PerkinElmer, U.S.) with an electron capture detector

(ECD) based on the U.S. Environmental Protection Agency methods 551 and 552.3.<sup>12,13</sup> Details are included in the Supporting Information (Text S4). Solid-phase extraction (SPE) was performed using Agilent Bond Elute PPL cartridges, and the recovery rate was 55.7 to 62.3%. After that, Fourier transform-ion cyclotron resonance–mass spectroscopy (FT-ICR-MS) analysis was conducted using a Bruker SolariX FT-ICR-MS instrument equipped with a 15.0 T superconducting magnet and an ESI ion source. The procedures for the SPE and FT-ICR-MS are available in the Supporting Information (Text S5).

**2.3. Data Analysis.** EEM data were handled (scattering eliminated, inner filter effect corrected, and intensity corrected) using R package Stadom,<sup>14</sup> and then, it was divided into five regions, and their integrals were calculated according to a previous study.<sup>15</sup> Principal component analysis (PCA) analysis were conducted using R package vegan. Other data processing and plotting are conducted on Origin 2018 and R 4.1.0.

### 3. RESULTS

**3.1. Bulk Characterization.** Total organic carbon (TOC), UV-vis spectra, EEM spectra, and SEC were used to evaluate the performance of three treatments from the bulk perspective and to determine the optimal dosage for the following investigation. The water qualities before and after different treatments is shown in Figure 1 and Figures S3–S5. PCA was used to provide an overview of three processes under different dosages (Figure 1a). Water indexes from EEM (integrated fluorescence intensity of five regions: R1–R5)<sup>15</sup> and UV-vis spectra (UV<sub>254</sub>) located at the positive side of the first principal axis could be seen. Along this axis, the JM and coagulation samples were clustered at the positive side, while oxidation and most adsorption samples were at the negative side. This indicated that coagulation had a poor removal of chromophore and fluorescent organic substances. On the opposite, ozone had high reactivity of ozone to unsaturated bonds and aromatic structures,<sup>16,17</sup> and therefore was effective in decreasing UV<sub>254</sub> and EEM intensity. As the dosage increases, the points of three treatments all shifted to a more negative side, indicating that the removal rate increased. TOC was located near the positive side of the second axis. It was noticed that adsorption showed the most significant decrease of TOC among three treatments. TOC removal by adsorption at the dosage of 50 mg/L already outperformed other two treatments at neutral conditions. Further increasing the PAC dose to 100 mg/L could reach a TOC removal rate of 37%. However, ozone had a limited effect on decreasing the organic content, with little changes in the TOC value even at the dosage of 2 mg/L (Figure S3a). This indicated that the oxidation effect of ozone was not able to achieve mineralization of the SMW-OM in this study.

The MW distribution was provided by SEC analysis, and there were three peaks, namely, peak1, peak2, and peak3, as shown in Figure 1b. Ozone showed a high reduction on peak1 and peak2, but little changes were observed for peak3 as the ozone concentration increases from 0.5 to 2 mg/L (Figure 1b), which was because of the degradation of high-MW substances to low-MW substances by ozonation. High-MW compounds were also easy to be removed by coagulation via sweep flocculation, and peak1 was more significantly decreased than peak2 and peak3 by coagulation (Figure 1b). For adsorption, the reduction of the three peaks was more even, with 38.1, 38.0, and 23.1% removal rates for peak1, peak2, and peak3 at the PAC dosage of 50 mg/L, respectively (Figure 1b). Therefore, adsorption not only outperformed the other two processes on TOC reduction but also showed better performance on the removal of substances with a relatively lower MW.

**3.2. DBP Formation Potential.** Based on the above bulk characterization, the specific water treatment conditions were selected for the following DBPFP measurements after adding chlorine at a concentration of three times the concentration of TOC and then keeping in a 20 °C incubator for 72 h. These

conditions were selected with the consideration of both effect and cost and were as follows: 1 mg/L ozone (OXI), 0.1 mM Al<sup>3+</sup> (COA), and 50 mg/L and 100 mg/L PAC (ADS-50 and ADS-100) for oxidation, coagulation, and adsorption, respectively. ADS-50 had a close TOC removal rate with COA (Figure 2a), and ADS-100 showed comparable removal of the chromophore and fluorescent organic substances with OXI (Figure 2g). UV<sub>254</sub>/TOC\*100 (SUVA) is an index to evaluate the aromatic content. As shown in Figure 2a, the SUVA of the OXI sample was the lowest among all samples, suggesting ozone preferentially transformed aromatic organic matter to aliphatic substances. Coagulation also favored the removal of aromatic structures, which were removed by the hydrophobic interaction with flocs. However, the decrease in SUVA by PAC was not as drastic as coagulation and adsorption, suggesting that adsorption had little priority for aromatic substances. According to EEM results (Figure 2b–f), fulvic acid-like substances (R3) and humic acid-like substances (R5) were two predominant EEM components, and the removal efficiency of EEM compounds followed OXI > ADS > COA (Figure 2g).

The performance of the three treatments on decreasing DBPFP is shown in Figures 2h, i and S6. It was noticed that the total DBP concentration followed OXI > JM > COA > ADS-50 > ADS-100, which can be partially explained by the TOC value, as shown in Figure 2a. However, the DBP yield (DBPs/TOC) also followed the same sequence, suggesting that the change in DBPFP after different treatments is related not only to the amount of total organic matter but also to the variation of organic composition. Previous studies used the variation of the EEM component to explain the change of DBPFP and suggested that DBPFP was significantly correlated fulvic-like (R3) and humic-like (RS) components.<sup>18</sup> This result might be true for water with a similar composition. For water samples after different treatments, the DOM composition varied significantly, and the EEM spectra could not be an effective technique to predict DBPFP. For instance, the OXI sample showed the best performance on the decrease of the EEM intensity, but the DBPFP of OXI sample was even higher than that of the raw water (JM).

As shown in Figures 2h, i, two kinds of trihalomethanes (THMs) [i.e., bromodichloromethane (BDCM) and trichloromethane (TCM)] and three kinds of haloacetic acids (HAAs) [i.e., chlorodibromoacetic acid (CDBA), dichloroacetic acid (DCAA), and bromodichloroacetic acid (BDCA)] were detected in water samples. It can be seen that the formation of THMs and HAAs after different treatments showed some differences. Specifically, the formation potential of THMs decreased as follows: OXI > JM > COA > ADS-50 > ADS-100, whereas the formation potential of HAAs was in the order JM > OXI > COA > ADS-50 > ADS-100. The results showed that adsorption achieved the lowest DBPFP. For 50 mg/L PAC, the formation potential of THMs and HAAs decreased to 57.61 and 34.74% of untreated water (JM samples), respectively, and these values further decreased to 42.67 and 27.92% for 100 mg/L PAC. Both THM and HAA formation potential decreased for the COA sample, while 1 mg/L ozone inhibited the HAA formation but promoted the THM formation. Previous studies also noticed this phenomenon, but little explanation had been suggested.<sup>19–21</sup> Considering that the mineralization effect of ozone was negligible, it was assumed that there was a transformation of HAA precursors to THM precursors during the ozone treatment. To further explore the

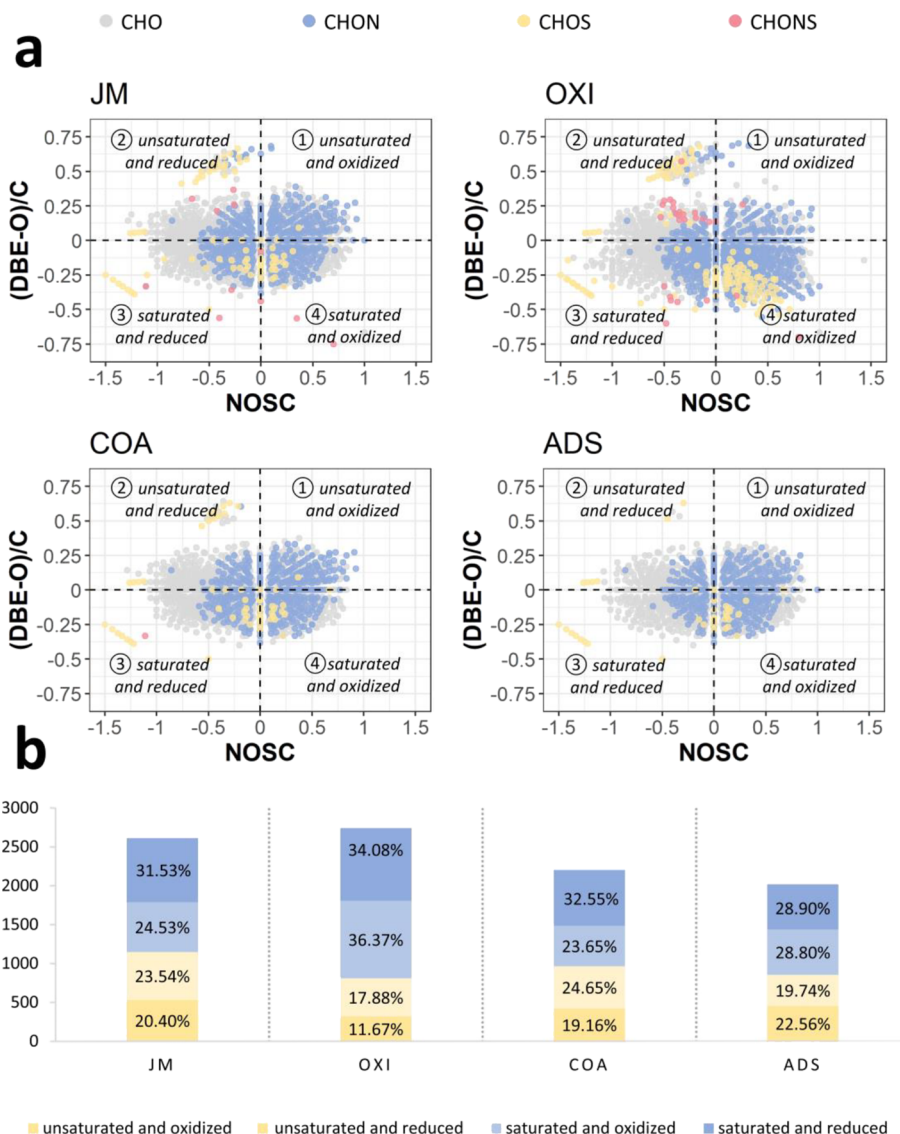


**Figure 3.** (a) (DBE-O)/C-NOSC plots of water samples before and after different treatments. The color indicates different subcategories: CHO, CHON, CHOS, CHONS, and the four quadrants indicate four states: (1) unsaturated and oxidized, (2) unsaturated and reduced, (3) saturated and reduced, (4) saturated and oxidized; (b) Bar diagrams showing the number and corresponding contribution percentage of molecules with different states in the four samples.

transformation processes, the FT-ICR-MS analysis was conducted in the following section.

**3.3. FT-ICR-MS Results.** After careful formula assignment for mass peaks with a signal to noise higher than 6 ( $S/N > 6$ ), formula values of 2122, 1772, 2296, and 1606 were determined for JM, COA, OXI, and ADS-50 (abbreviated as ADS) water samples, respectively. According to the results in Figure S7, the CHO-only component dominated the van Krevelen (VK) plot with >60% contribution in all samples. The second major subcategory was CHON components, and S-containing compounds only accounted for <8% of molecule numbers. However, for the OXI sample, an increase was observed in the number of S-containing compounds, which might be due to the transformation of one large molecule to several small molecules because S-containing groups are easy to react with ozone.<sup>22</sup>

Double bond equivalent minus oxygen per carbon ((DBE-O)/C) and nominal oxidation state of carbon (NOSC) are indexes that can be used to characterize the unsaturation and

oxidized states, respectively,<sup>23</sup> where larger positive values suggest a higher degree of unsaturation and oxidized state. Based on these two indexes, the molecules can be divided into four states: (1) unsaturated and oxidized, (2) unsaturated and reduced, (3) saturated and reduced, (4) saturated and oxidized, as shown in Figure 3a. The variations in the proportions of these four states are shown in Figure 3b. Both COA and ADS showed a reduction in molecule numbers, while OXI had more molecules than JM, suggesting that large molecules were degraded to several small molecules. In addition, there was significant transformation from the unsaturated state to the saturated state for OXI samples, with the proportion of the saturated state from 56.05 to 71.45%. However, very little change in the proportions of these four states was observed for the COA sample. As for the ADS sample, it was found that the proportion of reduced molecules decreased from 55.07 to 48.64%, indicating that adsorption might favor the removal of reduced components. When considering the change in molecule mass, adsorption out-

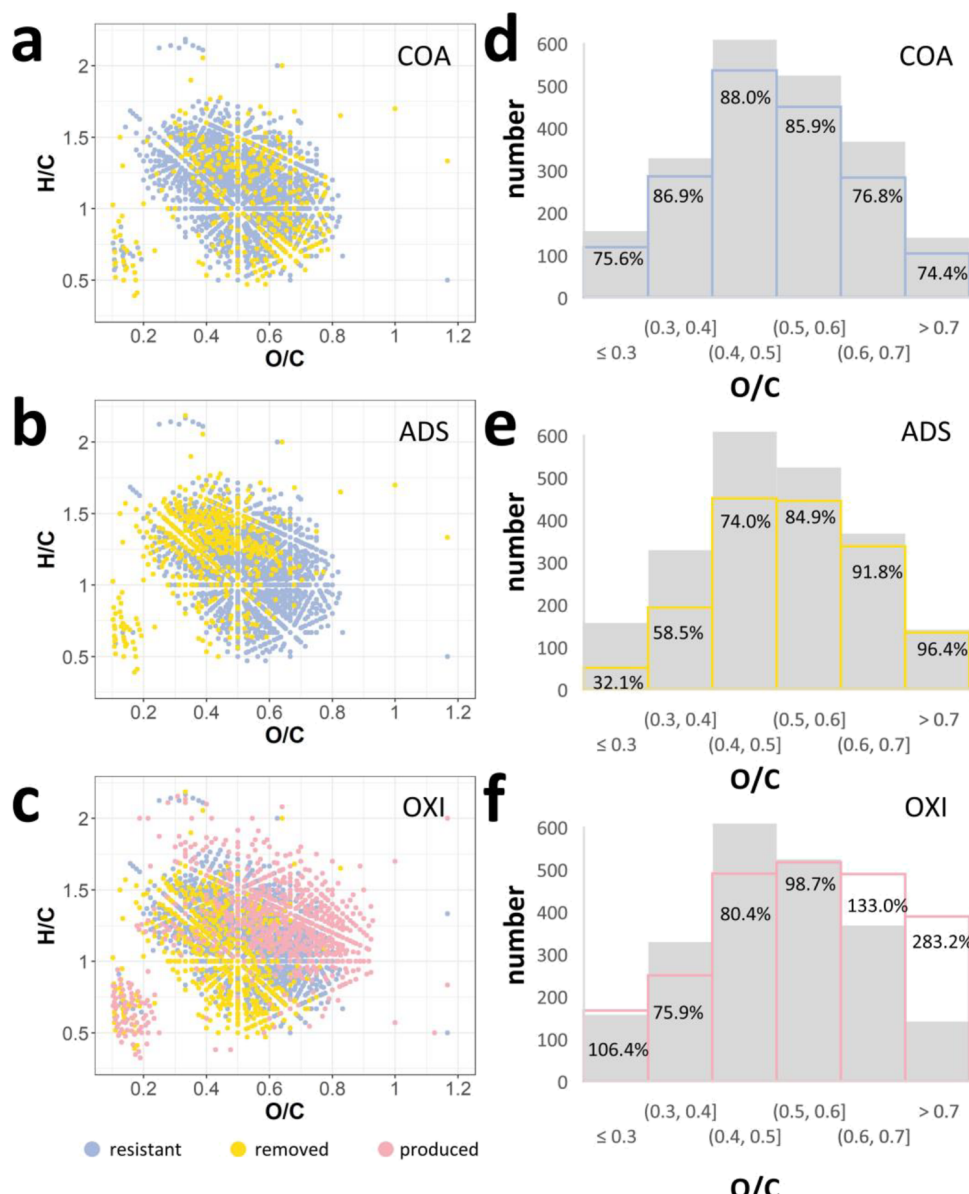


**Figure 4.** (a–c) Differentiated VK plot of COA (a), ADS (b), and OXI (c) samples. The colors of points indicate the type of molecules compared to raw water (JM): removed, produced, and resistant, and the shapes indicate the elemental composition: CHO, CHON, CHOS, and CHONS; (d–f) histogram showing the distribution of the O/C value for identified formulae in COA (d), ADS (e), and OXI (f) samples. Gray color represented the raw water (JM). The number indicates the percentage of molecule numbers after different treatments compared to JM.

performed coagulation on the removal of low-MW molecules, with 13% (ADS) and 4.8% (COA) removal rates for molecules with mass less than 300 Da (Figure S8).

To provide more intuitive information on the component variation during different treatments, the identified mass peaks of COA, ADS and OXI were compared with those of JM and divided into several types. Figure 4a–c depicts the differentiated van Krevelen (VK) plots of three samples. The blue points are molecules that were completely removed (i.e., molecules existed only in the JM water sample), while the gray points are resistant molecules (i.e., molecules existing in both), and the yellow ones are newly produced molecules (i.e., molecules not present in JM). It seemed that the removed molecules distributed randomly, as shown in Figure 4a, and coagulation had little selectivity on the molecules with different O/C and H/C (Figures 4d and S9). Previous studies suggested that coagulation preferentially removed compounds with high

O/C and low H/C,<sup>10,24</sup> which was only true for CHO molecules, as shown in Figure S10. Molecules with low H/C and high O/C were potentially aromatic structures with oxygen-containing groups (carboxyl and hydroxyl), which can adsorb onto alum flocs via hydrophobic<sup>25</sup> and electrostatic interactions.<sup>26</sup> However, for CHON compounds, molecules with high H/C ( $H/C > 1$ ) were preferentially removed. In addition, several molecules with a low O/C value ( $< 0.2$ ) were also found to be readily removed by coagulation, which might be because of their high mass and hydrophobicity.

As shown in Figure 4b, molecules removed by PAC adsorption mostly clustered at the top-left side of the VK plot, that is, were of low O/C and high H/C (Figures 4e and S9). Moreover, it was found that the removal rate decreased as the O/C value increases (67.9 and 3.6% for  $O/C < 0.3$  and  $> 0.7$ , respectively), suggesting that molecules with higher O/C were more difficult to be removed by adsorption. Generally,

molecules with higher O/C possibly carried more negative charges because of more oxygen-containing groups, such as hydroxyl and carboxyl groups. PAC used in this study was negatively charged (the zeta potential of 50 mg/L PAC solution was  $-24.8 \pm 0.2$  mV, pH 6.5), and thus, the electrostatic repulsion between PAC and these molecules reduces the likelihood of their adsorption.

Unlike coagulation and adsorption that only remove specific kinds of molecules from water, ozonation involves the chemical transformation of molecules. As discussed before, ozone, at typical doses, is unable to achieve significant mineralization of organic substances. Therefore, the molecules in OXI samples were into the following groups: removed, resistant, and produced. According to the VK plot in Figure 4c, the removed molecules were marked by lower O/C and H/C compared to the produced molecules (Figure 4f). It was noticed that a small number of molecules with low H/C ( $<1$ ) and low O/C ( $<0.3$ ) was produced (Figure 4c), which corresponds to condensed aromatic structures (CAS),<sup>27</sup> and was a result of the partial degradation of preexisting CAS in raw water. Previous studies have suggested that the unsaturated reduced fractions transform to saturated oxidized fractions during ozonation.<sup>23,28</sup> From the results in Figure 5, it was found that ozone increased

reactivity of saturated compounds with ozone is typically very low.<sup>16</sup> Although it is possible for these saturated molecules to be attacked by OH radicals, the consumption rate of OH radicals is usually lower than their formation rate.<sup>22</sup> Therefore, the unsaturated molecules were removed and saturated molecules accumulated during the ozonation process.

Recent studies have explored possible precursor–product pairs based on the mass difference analysis of several transformation reactions.<sup>23,29</sup> In our study, it was found that the reactions with the addition of O atoms (+O) and hydration (+H<sub>2</sub>O) possessed the two largest number of possible pairs among 15 reactions, as shown in the Supporting Information (Figure S13), which explained the obvious changes in O/C and the saturated state during ozonation. Figure S14a and S14b show the examples of possible precursor–product pairs for +1H<sub>2</sub>O and +1O. The change number (the number of O atoms or H<sub>2</sub>O that differs between products and products) was counted and is summarized in Figure S14e. It was observed that the H<sub>2</sub>O change number was less than 5 in most cases, while the change number for oxygen addition spread over a wider range. The most common reaction involving the addition of O atoms (+O) is hydroxylation at the aromatic ring, which is induced by a direct reaction with ozone or with ·OH radicals.<sup>30,31</sup> However, the addition of O atoms was also reported to break the benzene ring for some specific structures,<sup>32</sup> which contributed to the increase in the saturated state. An example of H<sub>2</sub>O addition reaction was when a secondary amine in the heterocycle was attacked by ozone, resulting in the cleavage of the N–C bond, with aldehyde formation after ring opening.<sup>33</sup>

#### 3.4. Molecule Transformation and DBP Formation.

Molecular insights can be obtained from the FT-ICR-MS results to explain the DBP formation potential after three treatments. For coagulation and adsorption that directly removed NOM from water, adsorption preferred to remove molecules with low O/C (reduced molecules), while coagulation aimed at more oxidized molecules (Figure S10). It is known that chlorine reactivity toward oxygenated moieties is usually limited, especially in the case of acid moieties that have high stability in the presence of chlorine.<sup>34</sup> Therefore, the reduced compounds removed by adsorption more readily react with HClO than oxidized compounds removed by coagulation. In other words, adsorption can remove more DBP precursors than coagulation, thus resulting in a lower DBPF. Moreover, adsorption can remove more molecules with small mass. For ozonation, on the one hand, molecules degraded from high-MW compounds increased the total amount of low-MW compounds. As the MW of the fractions decreased, the DBP yield coefficients increased.<sup>35</sup> On the other hand, ozonation increased the oxidized state and thus might decrease the reactivity with HClO. However, 1 mg/L ozone in this study only partially oxidized NOM, as was evidenced by more drastic variation in the unsaturated degree than the oxidized degree. The partially oxidized intermediate species can serve as DBP precursors. For instance, the reaction between olefins and ozone produced methyl ketones.<sup>36</sup> Organic matter with carbonyl functional groups (aldehyde or ketone) are major precursors of THMs, which react with chlorine via initial substitution reactions at the  $\alpha$ -carbon to the carbonyl group, followed by successive replacement of hydrogen with chlorine and subsequently produces acetate and chloroform via the haloform reaction.<sup>34</sup> Therefore, an increase in the THM formation potential was observed. Moreover, previous studies

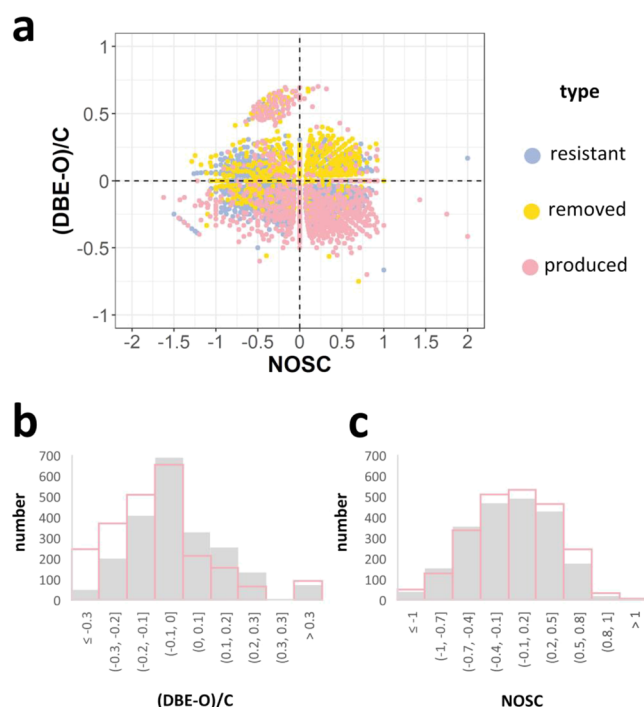


**Figure 5.** (a) Differentiated (DBE-O)/C-NOSC plot of the OXI sample. The colors of points indicate the type of molecules compared to raw water (JM): removed, produced, and resistant, and the shapes indicate the elemental composition: CHO, CHON, CHOS, and CHONS; (b, c) histogram showing the distribution of the (DBE-O)/C value (b) and the NOSC (c) value for identified formulae in the OXI sample. Gray color represented the raw water (JM).

the saturated state more significantly than the oxidized state at the dosage of 1 mg/L. That is, the removed and produced molecules were separated along the axis of DBE-O/C rather than NOSC. It was known that molecular ozone and OH radicals are the two oxidants present during ozonation.<sup>16</sup> Molecular ozone selectively reacts with structures such as double bonds and activated aromatic compounds, while their

have indicated that aliphatic structures resulted in more THM formation, while HAs had more aromatic structures as their precursors.<sup>26,37,38</sup> The significant reduction in the molecular unsaturated degree as well as the SUVA value suggested the decrease in aromatic components, and therefore, the HAA formation potential decreased during ozonation.

## 4. CONCLUSIONS

This study, for the first time, compared the performance of coagulation, oxidation, and adsorption on treating SMW-OM at the molecular scale, and their effects on decreasing DBP formation. The main conclusions were as follows:

- (1) Bulk characterization suggested that coagulation preferred the removal of high-MW and aromatic substances; ozonation had little mineralization effect on SMW-OM but exhibited an impressive reduction on chromophore and fluorescent organic substances. Adsorption showed effective reduction of TOC but seemed to have little priority on different SEC (MW) and EEM components.
- (2) CHO molecules with low H/C and high O/C were preferentially removed by coagulation. On the opposite, adsorption favored the removal of the low O/C (reduced) fraction. In addition, adsorption outperformed coagulation on removing low-MW molecules. As a result, adsorption had better performance on decreasing DBPFP than coagulation.
- (3) The variation on the molecular unsaturated degree was more significant than the oxidized degree during ozonation. Therefore, ozone transformed HAA precursors (aromatic matter) to THM precursors (aliphatic matter), thus resulting in the decrease in HAAFP and the increase in THMFP.

## ■ ASSOCIATED CONTENT

### Supporting Information

The Supporting Information is available free of charge at <https://pubs.acs.org/doi/10.1021/acsestengg.1c00409>.

Additional details for the coagulation (Text S1), adsorption (Text S2), and oxidation (Text S3) experiments; DBP measurement (Text S4) and the FT-ICR-MS analysis (Text S5). Calibration curve for the aqueous ozone concentration (Figure S1); water qualities of water samples treated by 200 mg/L PAC for different contact times (Figure S2); water quality indexes of water samples treated by oxidation (Figure S3), coagulation (Figure S4), and adsorption (Figure S5) under different dosages; DBP concentration and DBP yield (Figure S6); Van Krevelen (VK) diagrams and numbers of molecules with different elemental composition (Figure S7); distribution of the mass (Figure S8) and H/C (Figure S9) for identified formulae; differentiated VK plot (Figure S10); differentiated (DBE-O)/C-NOSC plot of the COA sample (Figure S11) and the ADS sample (Figure S12); number of possible precursor–product pairs of 15 different processes during oxidation (Figure S13); possible precursor–product pairs and the counts for +H<sub>2</sub>O and +O reactions (Figure S14). Molecular parameters (Table S1), indexes of water samples from FT-ICR-MS (Table S2), and properties of JingMi water (Table S3) ([PDF](#))

## ■ AUTHOR INFORMATION

### Corresponding Author

Wenzheng Yu – State Key Laboratory of Environmental Aquatic Chemistry, Key Laboratory of Drinking Water Science and Technology, Research Center for Eco-Environmental Sciences, Chinese Academy of Sciences, Beijing 100085, People's Republic of China; [orcid.org/0000-0001-9776-8021](https://orcid.org/0000-0001-9776-8021); Email: [wzyu@rcees.ac.cn](mailto:wzyu@rcees.ac.cn)

### Authors

Mengjie Liu – State Key Laboratory of Environmental Aquatic Chemistry, Key Laboratory of Drinking Water Science and Technology, Research Center for Eco-Environmental Sciences, Chinese Academy of Sciences, Beijing 100085, People's Republic of China; University of Chinese Academy of Sciences, Beijing 100049, People's Republic of China

Muhammad Saboor Siddique – State Key Laboratory of Environmental Aquatic Chemistry, Key Laboratory of Drinking Water Science and Technology, Research Center for Eco-Environmental Sciences, Chinese Academy of Sciences, Beijing 100085, People's Republic of China; University of Chinese Academy of Sciences, Beijing 100049, People's Republic of China

Nigel J. D. Graham – Department of Civil and Environmental Engineering, Imperial College London, London SW7 2AZ, U.K.

Complete contact information is available at:  
<https://pubs.acs.org/10.1021/acsestengg.1c00409>

### Notes

The authors declare no competing financial interest. All data needed to evaluate the conclusions in the manuscript are present in the manuscript and/or the Supplementary Materials. Additional data related to this study may be requested from the authors.

## ■ ACKNOWLEDGMENTS

This work was financially supported by the Beijing Natural Science Foundation (No. JQ21032) and the Key Research and Development Plan of the Chinese Ministry of Science and Technology (No. 2019YFD1100104 and No. 2019YFC1906501).

## ■ REFERENCES

- (1) Di Baldassarre, G.; Wanders, N.; AghaKouchak, A.; Kuil, L.; Rangecroft, S.; Veldkamp, T. I. E.; Garcia, M.; van Oel, P. R.; Breinl, K.; Van Loon, A. F. Water shortages worsened by reservoir effects. *Nat. Sustain.* **2018**, *1*, 617–622.
- (2) Byers, E. A.; Coxon, G.; Freer, J.; Hall, J. W. Drought and climate change impacts on cooling water shortages and electricity prices in Great Britain. *Nat. Commun.* **2020**, *11*, 2239.
- (3) Mekonnen, M. M.; Hoekstra, A. Y. Global Gray Water Footprint and Water Pollution Levels Related to Anthropogenic Nitrogen Loads to Fresh Water. *Environ. Sci. Technol.* **2015**, *49*, 12860–12868.
- (4) Tran, N. H.; Reinhard, M.; Gin, K. Y.-H. Occurrence and fate of emerging contaminants in municipal wastewater treatment plants from different geographical regions—a review. *Water Res.* **2018**, *133*, 182–207.
- (5) Su, Z.; Liu, T.; Li, X.; Graham, N.; Yu, W. Beneficial impacts of natural biopolymers during surface water purification by membrane nanofiltration. *Water Res.* **2021**, *201*, No. 117330.

- (6) Su, Z.; Liu, T.; Yu, W.; Li, X.; Graham, N. J. D. Coagulation of surface water: Observations on the significance of biopolymers. *Water Res.* **2017**, *126*, 144–152.
- (7) Amy, G.; Kuo, C.; Sierka, R. Ozonation of Humic Substances: Effects on Molecular Weight Distributions of Organic Carbon and Trihalomethane Formation Potential. *Ozone: Sci. Eng.* **2009**, *10*, 39–54.
- (8) Gibert, O.; Lefevre, B.; Fernández, M.; Bernat, X.; Paraira, M.; Pons, M. Fractionation and removal of dissolved organic carbon in a full-scale granular activated carbon filter used for drinking water production. *Water Res.* **2013**, *47*, 2821–2829.
- (9) Lavonen, E. E.; Kothawala, D. N.; Tranvik, L. J.; Gonsior, M.; Schmitt-Kopplin, P.; Köhler, S. J. Tracking changes in the optical properties and molecular composition of dissolved organic matter during drinking water production. *Water Res.* **2015**, *85*, 286–294.
- (10) Yuan, Z.; He, C.; Shi, Q.; Xu, C.; Li, Z.; Wang, C.; Zhao, H.; Ni, J. Molecular Insights into the Transformation of Dissolved Organic Matter in Landfill Leachate Concentrate during Biodegradation and Coagulation Processes Using ESI FT-ICR MS. *Environ. Sci. Technol.* **2017**, *51*, 8110–8118.
- (11) Roth, V.-N.; Lange, M.; Simon, C.; Hertkorn, N.; Bucher, S.; Goodall, T.; Griffiths, R. I.; Mellado-Vázquez, P. G.; Mommer, L.; Oram, N. J.; Weigelt, A.; Dittmar, T.; Gleixner, G. Persistence of dissolved organic matter explained by molecular changes during its passage through soil. *Nat. Geosci.* **2019**, *12*, 755–761.
- (12) EPA, U. S. Method 551.1: Determination of Chlorination Disinfection Byproducts, Chlorinated Solvents, and Halogenated Pesticides/Herbicides in Drinking Water by Liquid-Liquid Extraction and Gas Chromatography With Electron-Capture Detection, Revision 1.0. Cincinnati, OH, **1995**.
- (13) EPA, U. S. Method 552.3: Determination of haloacetic acids and dalapon in drinking water by liquid-liquid microextraction, derivatization, and Gas chromatography with electron capture detection. EPA 815-B-03-002. Revision 1.0, **2003**.
- (14) Pucher, M.; Wünsch, U.; Weigelhofer, G.; Murphy, K.; Hein, T.; Graeber, D. staRdom: Versatile Software for Analyzing Spectroscopic Data of Dissolved Organic Matter in R. *Water* **2019**, *11*, 2366.
- (15) Park, M.; Snyder, S. A. Sample handling and data processing for fluorescent excitation-emission matrix (EEM) of dissolved organic matter (DOM). *Chemosphere* **2018**, *193*, 530–537.
- (16) Von Sonntag, C.; Von Gunten, U. *Chemistry of Ozone in Water and Wastewater Treatment: From Basic Principles to Applications*; IWA Publishing, 2012.
- (17) Phungsai, P.; Kurisu, F.; Kasuga, I.; Furumai, H. Molecular characteristics of dissolved organic matter transformed by O<sub>3</sub> and O<sub>3</sub>/H<sub>2</sub>O<sub>2</sub> treatments and the effects on formation of unknown disinfection by-products. *Water Res.* **2019**, *159*, 214–222.
- (18) Xu, X.; Kang, J.; Shen, J.; Zhao, S.; Wang, B.; Zhang, X.; Chen, Z. EEM-PARAFAC characterization of dissolved organic matter and its relationship with disinfection by-products formation potential in drinking water sources of northeastern China. *Sci. Total Environ.* **2021**, *774*, No. 145297.
- (19) Gallard, H.; von Gunten, U. Chlorination of natural organic matter: kinetics of chlorination and of THM formation. *Water Res.* **2002**, *36*, 65–74.
- (20) Duan, X.; Liao, X.; Chen, J.; Xie, S.; Qi, H.; Li, F.; Yuan, B. THMs, HAAs and NAs production from culturable microorganisms in pipeline network by ozonation, chlorination, chloramination and joint disinfection strategies. *Sci. Total Environ.* **2020**, *744*, No. 140833.
- (21) Zhou, S.; Zhu, S.; Shao, Y.; Gao, N. Characteristics of C-, N-DBPs formation from algal organic matter: Role of molecular weight fractions and impacts of pre-ozonation. *Water Res.* **2015**, *72*, 381–390.
- (22) Von Gunten, U. Ozonation of drinking water: Part I. Oxidation kinetics and product formation. *Water Res.* **2003**, *37*, 1443–1467.
- (23) Zhang, B.; Shan, C.; Wang, S.; Fang, Z.; Pan, B. Unveiling the transformation of dissolved organic matter during ozonation of municipal secondary effluent based on FT-ICR-MS and spectral analysis. *Water Res.* **2021**, *188*, No. 116484.
- (24) Riedel, T.; Biester, H.; Dittmar, T. Molecular Fractionation of Dissolved Organic Matter with Metal Salts. *Environ. Sci. Technol.* **2012**, *46*, 4419–4426.
- (25) Galindo, C.; Del Nero, M. Chemical fractionation of a terrestrial humic acid upon sorption on alumina by high resolution mass spectrometry. *RSC Adv.* **2015**, *5*, 73058–73067.
- (26) Zhang, H.; Zhang, Y.; Shi, Q.; Ren, S.; Yu, J.; Ji, F.; Luo, W.; Yang, M. Characterization of low molecular weight dissolved natural organic matter along the treatment trait of a waterworks using Fourier transform ion cyclotron resonance mass spectrometry. *Water Res.* **2012**, *46*, 5197–5204.
- (27) Ohno, T.; He, Z.; Sleighter, R. L.; Honeycutt, C. W.; Hatcher, P. G. Ultrahigh Resolution Mass Spectrometry and Indicator Species Analysis to Identify Marker Components of Soil- and Plant Biomass-Derived Organic Matter Fractions. *Environ. Sci. Technol.* **2010**, *44*, 8594–8600.
- (28) Phungsai, P.; Kurisu, F.; Kasuga, I.; Furumai, H. Molecular characterization of low molecular weight dissolved organic matter in water reclamation processes using Orbitrap mass spectrometry. *Water Res.* **2016**, *100*, 526–536.
- (29) Schollée, J. E.; Bourgin, M.; von Gunten, U.; McArdell, C. S.; Hollender, J. Non-target screening to trace ozonation transformation products in a wastewater treatment train including different post-treatments. *Water Res.* **2018**, *142*, 267–278.
- (30) Tay, K. S.; Rahman, N. A.; Abas, M. R. B. Ozonation of parabens in aqueous solution: Kinetics and mechanism of degradation. *Chemosphere* **2010**, *81*, 1446–1453.
- (31) Hübner, U.; Seiwert, B.; Reemtsma, T.; Jekel, M. Ozonation products of carbamazepine and their removal from secondary effluents by soil aquifer treatment – Indications from column experiments. *Water Res.* **2014**, *49*, 34–43.
- (32) Mawhinney, D. B.; Vanderford, B. J.; Snyder, S. A. Transformation of 1H-Benzotriazole by Ozone in Aqueous Solution. *Environ. Sci. Technol.* **2012**, *46*, 7102–7111.
- (33) Borowska, E.; Bourgin, M.; Hollender, J.; Kienle, C.; McArdell, C. S.; von Gunten, U. Oxidation of cetirizine, fexofenadine and hydrochlorothiazide during ozonation: Kinetics and formation of transformation products. *Water Res.* **2016**, *94*, 350–362.
- (34) Deborde, M.; von Gunten, U. Reactions of chlorine with inorganic and organic compounds during water treatment—Kinetics and mechanisms: A critical review. *Water Res.* **2008**, *42*, 13–51.
- (35) Gang, D.; Clevenger, T. E.; Banerji, S. K. Relationship of chlorine decay and THMs formation to NOM size. *J. Hazard. Mater.* **2003**, *96*, 1–12.
- (36) Von Gunten, U. Ozonation of drinking water: Part II. Disinfection and by-product formation in presence of bromide, iodide or chlorine. *Water Res.* **2003**, *37*, 1469–1487.
- (37) Liang, L.; Singer, P. C. Factors Influencing the Formation and Relative Distribution of Haloacetic Acids and Trihalomethanes in Drinking Water. *Environ. Sci. Technol.* **2003**, *37*, 2920–2928.
- (38) Hua, G.; Reckhow, D. A. Characterization of Disinfection Byproduct Precursors Based on Hydrophobicity and Molecular Size. *Environ. Sci. Technol.* **2007**, *41*, 3309–3315.